

CONTROL OF THE WEAKLY DAMPED SYSTEM WITH THE EMBEDDED SYSTEM SUPPORT

Marek PASKALA, Jozef SEDO, Anna KONDELOVA

¹Department of Mechatronics and Electronic, Faculty of Electrical Engineering, University of Zilina, Univerzitna 8215/1, 01026 Zilina, Slovak Republic

marek.paskala@fel.uniza.sk, jozef.sedo@fel.uniza.sk, anna.kondelova@fel.uniza.sk

DOI: 10.15598/aece.v16i4.2878

Abstract. This paper deals with the experimental verification of the importance of embedded systems with an applied MEMS sensor in controlling weakly damped systems. The aim is to suppress actively residual oscillations. The model of a planar physical pendulum with a prismatic joint was chosen for the experiment. The sensor made by MEMS technology, in which three-axis gyroscope and three-axis accelerometer are integrated, has been used for sensing the angle of deflection of the load from the equilibrium position. The simulation model represents the crane arm with a moving carriage.

proach has a weak point in the event of residual vibrations, for example, due to the action of an insufficient quantity. The solution described in the paper is based on MEMS sensor application. On the basis of the measured values, the control system determines the magnitude of the correction quantity in real time. Applying the correction manipulated variable actively reduces residual vibrations. The physical model of a weakly damped system consisting of a carriage with pendulum was selected to verify the importance of applying the correction variable.

Keywords

Active damping, control of damping, residual oscillations.

1. Introduction

Control of weakly damped systems has its own specifics. With these systems, residual vibrations occur. The issue of controlling weakly damped systems is still up to date and with new technological options, there is an opportunity to apply new approaches to control such systems. Today, several methods designed to reduce system oscillation are known [1]. Some methods are based on a change in the character of a closed control system in the manner that the damping coefficient increases. Achieving this goal is possible by the correct setting of the controller or adding acceleration feedback. Another possibility is the use of control signal shapers [2] and [3]. This method preserves the weakly damped character of the system. All the above-mentioned control methods have in common aim of suppressing residual vibrations. However, this ap-

2. Dynamic Structure

The creating of the mathematical model of a mechanical system is based on the number of degrees of freedom. The number of degrees of freedom of the mechanism was chosen by calculation for the selected model. For the chosen planar case it is $n = 2^\circ$. Based on the number of degrees of freedom, it is known that the model has two generalized coordinates, and therefore it will be described by two motion equations.

The angular dependencies expressed from the geometry of the mechanism are:

$$\cos \varphi = \frac{y_{21}}{l}, \quad \cos \varphi = \frac{y_1 - y_2}{l}, \quad (1)$$

$$\sin \varphi = \frac{x_{21}}{l}, \quad \sin \varphi = \frac{x_1 - x_2}{l}, \quad (2)$$

and other geometrically dependent equations:

$$x_2 = x_1 - l \sin \varphi, \quad (3)$$

$$y_2 = y_1 - l \cos \varphi. \quad (4)$$

Expression of kinetic E_k and potential E_p energy of investigated system is:

$$E_k = \frac{1}{2}m_1v_1^2 + \frac{1}{2}m_2v_2^2 = \frac{1}{2}m_1\dot{x}_1 + \frac{1}{2}m_2(\dot{x}_2^2 + \dot{y}_2^2), \quad (5)$$

$$E_p = m_1gy_1 + m_2gy_2 = m_1gy_1 + m_2g(y_1 - l \cos \varphi), \quad (6)$$

after the solution comes:

$$E_k = \frac{1}{2}(m_1 + m_2)\dot{x}_1^2 - m_2\dot{x}_1\dot{\varphi} \cos \varphi + \frac{1}{2}m_2l^2\dot{\varphi}^2, \quad (7)$$

$$E_p = (m_1 + m_2)gy_1 - m_2gl \cos \varphi. \quad (8)$$

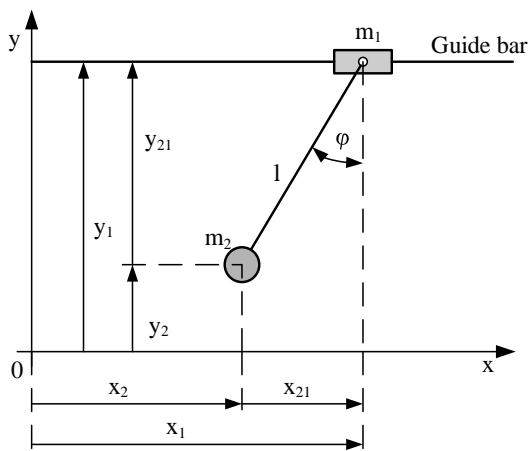


Fig. 1: Dynamic diagram of the mechanical system.

2.1. Lagrange's Equations of the Second Kind

Lagrange's equations of the second kind are applied to both derived generalized coordinates (φ, x) . Lagrange's equations of the second type have a form:

$$\frac{d}{dt} \left(\frac{\partial E_k}{\partial \dot{q}_j} \right) - \frac{\partial E_k}{\partial q_j} = - \frac{\partial E_p}{\partial q_j}, \quad j = 1, 2, \dots, n. \quad (9)$$

The final form of motion equations for the mechanism being investigated is:

$$\ddot{\varphi} = \frac{1}{l}(\ddot{x}_1 \cos \varphi - g \sin \varphi), \quad (10)$$

$$\ddot{x}_1 = \frac{m_2}{m_1 + m_2}l(\ddot{\varphi} \cos \varphi - \dot{\varphi}^2 \sin \varphi). \quad (11)$$

When considering damping or dissipative forces, Lagrange's equations of the second kind are:

$$\frac{d}{dt} \left(\frac{\partial E_k}{\partial \dot{q}_j} \right) - \frac{\partial E_k}{\partial q_j} = - \frac{\partial E_p}{\partial q_j} - \frac{\partial D}{\partial \dot{q}_j}, \quad j = 1, 2, \dots, n. \quad (12)$$

The resulting equation after the inclusion of resistive forces to the motion equations is followed by:

$$\ddot{\varphi} = \frac{1}{l}(\ddot{x}_1 \cos \varphi - g \sin \varphi) \pm \frac{F_\varphi}{m_2l^2}, \quad (13)$$

$$\ddot{x}_1 = \frac{m_2}{m_1 + m_2}l(\ddot{\varphi} \cos \varphi - \dot{\varphi}^2 \sin \varphi) \pm \frac{F_\varphi \cos \varphi + F_x l}{(m_1 + m_2 \sin^2 \varphi)l}. \quad (14)$$

3. Transfer Function

The transfer function is expressed from the differential equation that describes the selected weakly damped system. The differential equation is derived from the torque condition. The assumption of a strong positional feedback has been introduced to exclude the transfer of the reaction force from the load on the carriage [4]. It allows the system to be investigated as one mass.

$$J_Z \ddot{\varphi} + B_Z \dot{\varphi} + mlg \sin \varphi = -ml \cos \varphi a. \quad (15)$$

The obtained differential equation is linearized because Laplace's transformation can only be used to solve linear differential equations with constant coefficients. For small displacements of the load, the following applies:

$$\sin \varphi = \varphi, \quad (16)$$

$$\cos \varphi = 1. \quad (17)$$

After applying the simplification, the acquired equation is:

$$J_Z \ddot{\varphi} + B_Z \dot{\varphi} + mlg \varphi = -mla. \quad (18)$$

The differential equation has been transformed by Laplace's vocabulary:

$$J_Z s^2 \phi + B_Z s \phi + mlg \phi = -mlA. \quad (19)$$

Subsequently, the transfer is obtained as a ratio of the output quantity image and the input quantity image:

$$F(s) = \frac{\phi}{A} = \frac{-\frac{ml}{J_Z}}{s^2 + s \frac{B_Z}{J_Z} + \frac{mlg}{J_Z}}. \quad (20)$$

After edition, the transfer function is:

$$F(s) = \frac{-\frac{1}{g}\omega_0^2}{s^2 + 2s\omega_0 b + \omega_0^2}. \quad (21)$$

Finally, the following substitutions may be introduced:

$$K = -\frac{1}{g}, \tag{22}$$

$$b = -\frac{B_Z}{2J_Z\omega_0}, \tag{23}$$

$$\omega_0^2 = \frac{mgl}{J_Z}. \tag{24}$$

Provided the heavy load, the moment of inertia J_Z can be expressed as:

$$J_Z = ml^2. \tag{25}$$

After substitution of the relation Eq. (25) to Eq. (24), the natural frequency is:

$$\omega_0^2 = \frac{g}{l}. \tag{26}$$

The Bode diagram for the transfer function Eq. (21) is shown in Fig. 2 [7]. For the calculation, values corresponding to the experimental system were used; $g = 9.81 \text{ m}\cdot\text{s}^{-2}$; $l = 0.77 \text{ m}$; $m = 0.138 \text{ kg}$; $B_Z = 0.00008$. On the amplitude characteristic, it is clear to see that the examined system has a resonant frequency of $3.57 \text{ rad}\cdot\text{s}^{-1}$, which is 0.568 Hz .

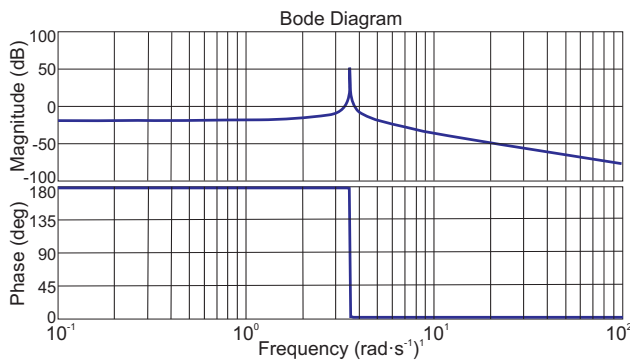


Fig. 2: Bode diagram.

4. Simulation Analysis of the System

The simulation model of the mechanical system has been created in the Matlab Simulink environment. The environment allows simple modification of the mechanical system model parameters (dimensions, friction forces, load weight change, etc.). At the same time, it allows the introduction of a control loop into the model [8]. To create a mechanical model, the Sim-Mechanic library was used. The simulation model of the mechanism is shown in Fig. 3. The simulation outputs from the Matlab Simulink model were compared

with motion equations derived in the previous chapter. In this way, the correctness of the mechanical model created in the Matlab Simulink environment was verified. Movement of the mechanism during the simulation is allowed by the Mechanics Explorers graphical interface Fig. 4.

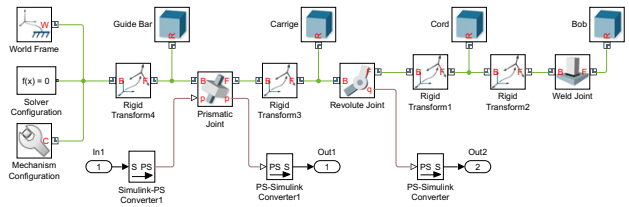


Fig. 3: Model of the mechanism created in the Matlab Simulink environment.

The next step was the design and incorporation of the position control. A control loop with PI controller application was used. The priority of control is to position the load at the desired location with suppression of residual oscillations [9].

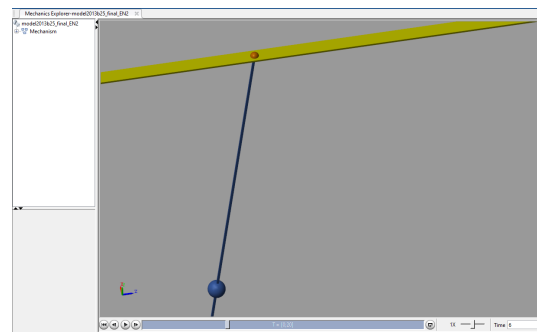


Fig. 4: Graphic presentation of mechanism in Mechanics Explorers.

The output of the rotational joint of the model of the mechanism directly provides the position of the trolley, as well as the actual angle of deflection of the load as seen from Fig. 3. In Fig. 5, there is a view on the overall simulation scheme. The complete model of the mechanical system, whose structure is shown in Fig. 3, is in the subsystem Mechanism. This subsystem has one input In1 for input of the manipulated variable and two outputs Out1 and Out2. Out1 is the output of the carriage position. Out2 is the output of the deflection of the load from the equilibrium state. The second subsystem, called Embedded system, represents the load-displacement evaluation system. Its input In1 is provided with information about the angle of deflection of the load. Output Out1 is an additional correction value. The source is used to generate a change in the desired location over time. The summation element calculates the control deviation that enters the PI controller. Proportional constant $P = 0.05$ and integration constant $I = 1.4$. The following blocks

are derivative block and saturation block. Limitations have been set with saturation blocks. The speed is limited to $4.6 \text{ m}\cdot\text{s}^{-1}$ and acceleration to $100 \text{ m}\cdot\text{s}^{-2}$.

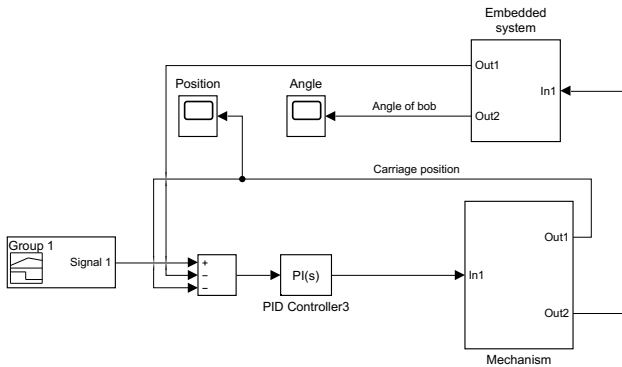


Fig. 5: Simulation diagram with mechanical model, position control and applied embedded system.

In the next, the load-displacement evaluation system will be called an embedded system. The behavior of the system without an embedded system and subsequently with the applied embedded system was tested by simulations. The following results were obtained.

Graphical waveforms obtained from the simulation without using the embedded system are listed as the first. The graphical dependence of the system response to changing the setpoint of the carriage (position) is in Fig. 6. The residual vibrations are shown in Fig. 7.

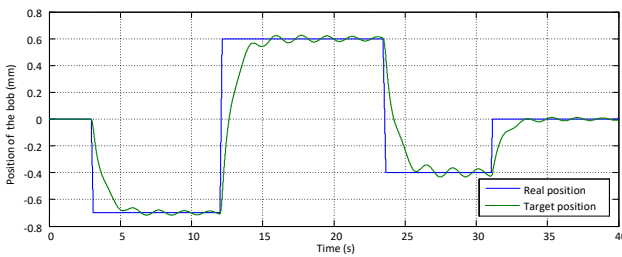


Fig. 6: Steering of carriage position without regulation of oscillations by embedded system.

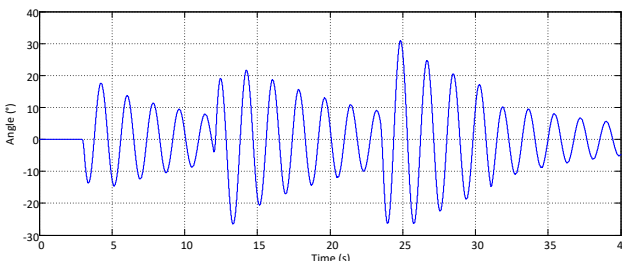


Fig. 7: The oscillation of the load in the desired position.

The waveform of the action variable of acceleration, as well as the speed, can be read from the graph in Fig. 8. The acceleration waveform can be seen from

the graph. The entire range -100 to $+100 \text{ m}\cdot\text{s}^{-2}$ is not plotted due to the better readability of the graphical waveform of the acceleration. The acceleration pulses reached preset saturation.

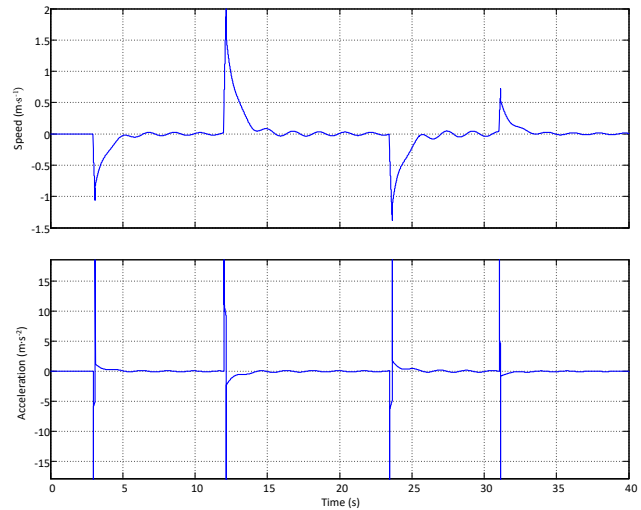


Fig. 8: Course of manipulated variable at steering of position.

The graphical waveforms obtained from the simulation after connecting the embedded system showed visible acceleration of the load oscillation stabilization at the desired position, Fig. 10. The embedded system, which with its added value implemented additional motion control of the carriage, has ensured that the vibration stop time was shortened. This can also be seen from the placement of the carriage to the desired position in Fig. 9.

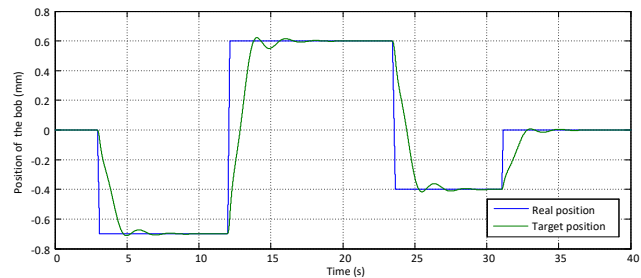


Fig. 9: Control of carriage position with regulation of oscillations by embedded system.

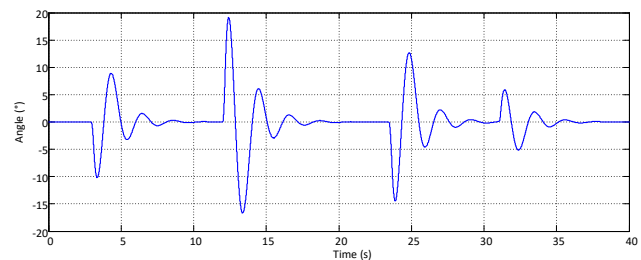


Fig. 10: The oscillation of the load in the desired position.

The waveform of the action variable during the control is shown in Fig. 11.

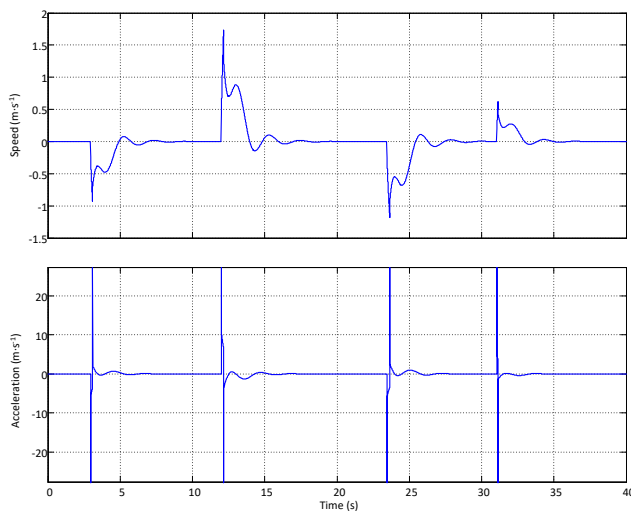


Fig. 11: Course of manipulated variable at steering of position and simultaneous active damping.

Functionality of the implemented embedded system has been tested with modified parameters of the mechanical system. The weight of the load and the length of the bar link were changed. In all tested cases, the model with applied embedded system achieved a significant shortening of the stop time of the load in the desired position compared to the model where the embedded system was not applied.

5. Experimental Verification

Construction from aluminium profiles is the basis of an experimental device. A moving carriage, which is driven by a DC motor via a toothed belt, is mounted on the top of the structure. The position of the carriage is read off from the rotary encoder located on the motor. The load is placed on a 1m long rotatable rod that is mounted to the carriage. The sensor of the angle of load tilt is on the rod at the point of rotational joint of the rod to the carriage. It is a MEMS sensor that has an integrated three-axis gyroscope and a three-axis accelerometer [10]. Data from the sensors is fed to the input/output unit of the DSpace system, in which is the program compiled from the Matlab environment. Through the Control Desk software, it is possible to monitor and correct the control process.

Control of the experimental assembly was performed through the Matlab Simulink program and the dSpace interface. In the Matlab Simulink environment, a basic control loop for control of the carriage position was created in the first step [5]. The block of the PI controller and the PWM block were used. Subsequently, an embedded system was programmed to communicate

with the MEMS sensor through the serial line [6]. The structure of the control program is in Fig. 13.

The experimental device was connected to the input/output interface of dSpace. Through the Control Desk interface, the control process was evaluated.

5.1. Experiment Evaluation

The first step was to optimize the constants of PI controller of position control loop. Controller constants $P = 0.001$ and $I = 0.01$ were determined by applying the Ziegler-Nichols method [7]. Data from the MEMS sensor was decoded and corrected in the dSpace system. The processed data was used in the block representing the embedded system to calculate the correction variable. The output from this block was brought to the summation element, where the correction value is subtracted from the desired position, see Fig. 13. This method was chosen to not interfere with the control loop of a position, but only to correct the setpoint. Subsequently, the embedded system was debugged and experimental measurements were performed.

From the realized experiments, the representative samples of measurements were selected, on which the impact of the embedded system at the attenuation of residual oscillation will be presented.

The measurement records on the model without application of the embedded system are listed first. Because of the comparability of the results, measurements were always run from a steady state. For the action, the unshaped control signal was used because it was not intended to prevent the occurrence of residual oscillations at start-up, but to ensure that the load stays in the desired position in the shortest possible time. Figure 12 shows the system response to a step change of the desired position and the control of the system with a control deviation approaching zero.

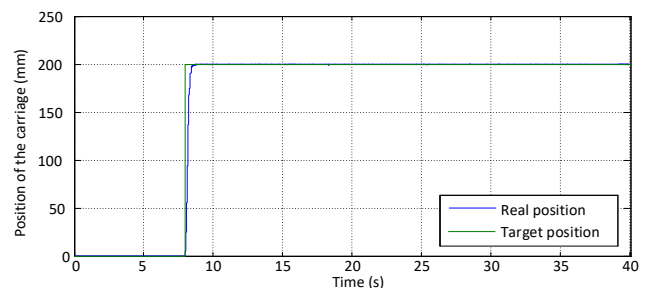


Fig. 12: Time course of carriage deployment without active damping.

Figure 14 shows the system response in the form of residual oscillations as well as the real magnitude of the attenuation without application of the embedded system, whose role is to ensure active damping. The

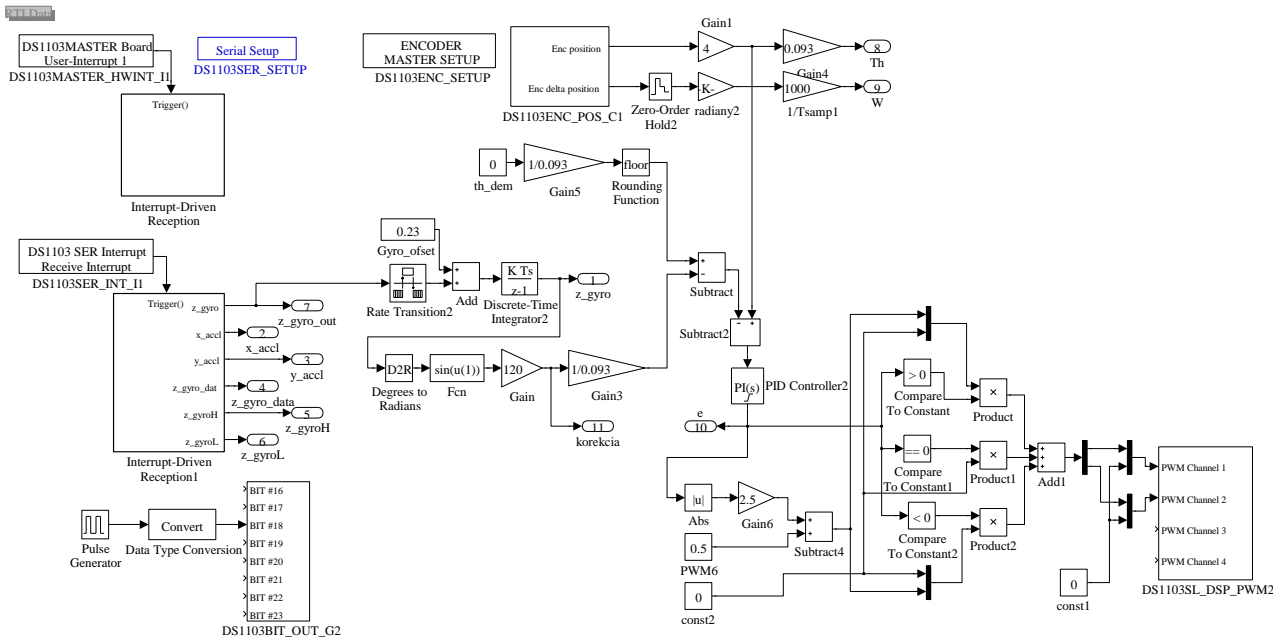


Fig. 13: Basic control loop with implemented embedded system in Matlab Simulink environment.

size of the logarithmic decrement of attenuation δ was determined by the calculation. Logarithmic decrement of the used model is $\delta = 9.9 \cdot 10^{-3}$.

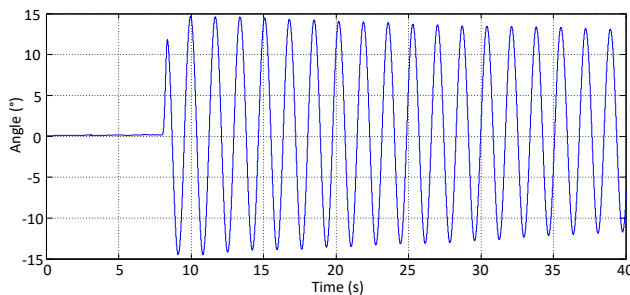


Fig. 14: Course of the load oscillation without active damping.

After identifying the behavior of an experimental model without an applied embedded system, experiments were carried out on a model with an applied embedded system whose task was active damping of residual oscillations. The parametrically identical jump change of the desired position was used as in the system without the applied embedded system. On the waveform of position in Fig. 15, the movement of the carriage about the desired position during active damping is clearly shown.

The steady state of the system, as mentioned above, did not occur, but the controller oscillated around the desired position that was influenced by the embedded system. It can also be seen from the waveform of the control variable from the PI regulator providing position control, Fig. 16.

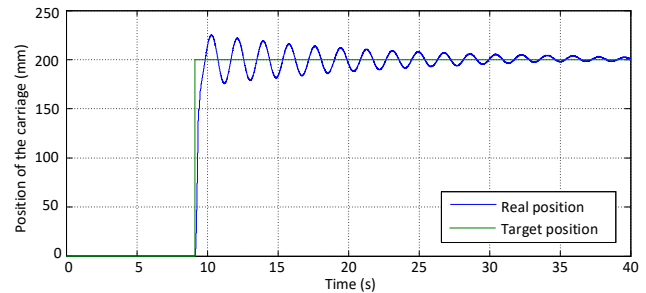


Fig. 15: Time waveform of carriage position with active damping.

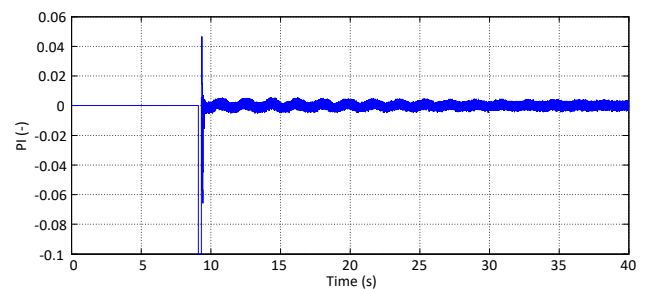


Fig. 16: Position control with active damping - output from the PI controller.

As in the previous case, the logarithmic decrement of the attenuation δ was calculated. The logarithmic decrement of the system with active damping is $\delta = 136 \cdot 10^{-3}$. For a better comparison, the system response without active damping and system response using the active damping provided by the embedded system is plotted in one chart. The importance of the application of the embedded system in

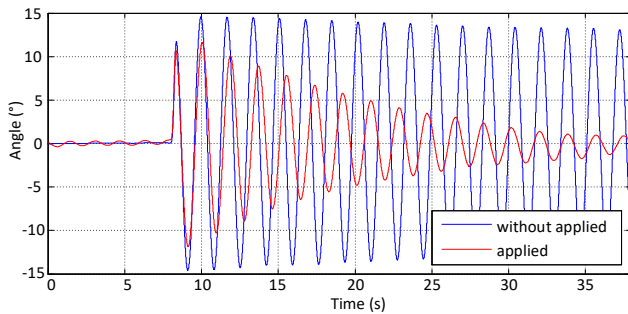


Fig. 17: Position control, comparison of weakly damped oscillation with application of controlled damping.

the area of active damping of weakly damped systems can be justified by the results of the experiments. The time required to stabilize residual oscillations was decreased by 13.7 times. All options to further increases in attenuation are not yet exhausted. As can be seen from the start of the carriage to the desired position and from the standard course of residual oscillations (Fig. 18), the embedded system has been unable to intervene more effectively under these conditions. Reducing the steadying time would be possible by increasing the power of the drive for the experimental model.

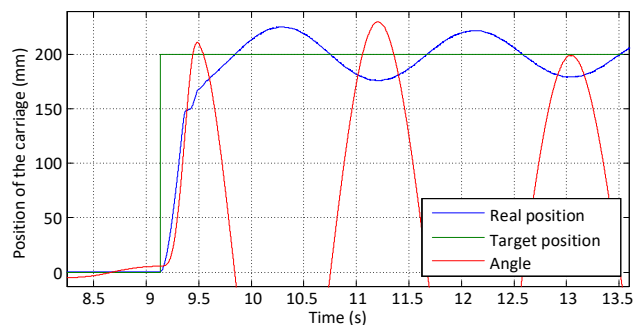


Fig. 18: Dependence of system dynamics and frequency of residual oscillations.

6. Conclusion

In order to verify the importance of application of the embedded system with the MEMS sensor in the control of weakly damped systems, a model of a planar physical pendulum with a prismatic joint was chosen. Motion equations for the selected model were derived. Simulation model in Matlab Simulink was created, on which the correctness of the proposed solution has been verified by simulations. Finally, the importance of application of the embedded system with a MEMS sensor for the improvement of the quality of control of weakly damped systems was experimentally verified.

In conclusion, it is still necessary to point out that the proposed system does not aim to replace the used

signal shapers whose task is to ensure the start and run without load oscillations [11]. The significance of the embedded system with a MEMS sensor can be seen in increasing the robustness of the system in cooperation with the shapers.

The achieved results and graphs show a significant improvement in the load movement regulation. The oscillation stabilization occurred 13.7 times faster than the control without the embedded system. In the simulation, the impact on attenuation of residual oscillations was even more pronounced.

When designing an embedded system, emphasis was placed on its technical feasibility, the possibility of application to existing real systems.

Acknowledgment

This paper is supported by the following project: APVV 0396-15, KEGA 073ZU-4/2017.

References

- [1] VAZQUEZ, C. and J. COLLADO. Oscillation attenuation in an overhead crane: comparison of some approaches. In: *2009 6th International Conference on Electrical Engineering, Computing Science and Automatic Control (CCE)*. Toluca: IEEE, 2009, pp. 1–6. ISBN 978-1-4244-4688-9. DOI: 10.1109/ICEEE.2009.5393418.
- [2] GNIADK, M. Usage of input shaping for crane load oscillation reduction. In: *2015 20th International Conference on Methods and Models in Automation and Robotics (MMAR)*. Miedzyzdroje: IEEE, 2015, pp. 278–282. ISBN 978-1-4799-8701-6. DOI: 10.1109/MMAR.2015.7283887.
- [3] HOFFMANN, C., C. RADISCH and H. WERNER. Active Damping of Container Crane Load Swing by Hoisting Modulation – An LPV Approach. In: *2012 IEEE 51st IEEE Conference on Decision and Control (CDC)*. Maui: IEEE, 2012, pp. 5140–5145. ISBN 978-1-4673-2066-5. DOI: 10.1109/CDC.2012.6426889.
- [4] LAWRENEC, W. J. *Crane Oscillation Control: Nonlinear Elements and Educational Improvements*. Atlanta, Dissertation. George W. Woodruff School. Supervisor Dr. William Singhose.
- [5] KARBAN, P. *Vypočty a simulace v programech Matlab a Simulink*. 1st ed. Brno: Computer Press, 2006. ISBN 978-80-251-1448-3.

- [6] DUCHON, F. and A. BABINEC. *Lokalizacia mobilnych robotov*. 1st ed. Bratislava: Slovenska technicka univerzita v Bratislave, 2015. ISBN 978-80-227-4461-4.
- [7] BALATE, J. *Automaticke rizeni*. 1st ed. Prague: BEN, 2003. ISBN 80-7300-020-2.
- [8] URICA, T., A. SIMONOVA and S. KASCAK. Control systems design and simulation of continuous systems. In: *2017 18th International Scientific Conference on Electric Power Engineering (EPE)*. Kouty nad Desnou: IEEE, 2017, pp. 1–5. ISBN 978-1-5090-6406-9. DOI: 10.1109/EPE.2017.7967263.
- [9] VAUGHAN, J., A. KARAJGIKAR and W. SINGHOSE. A study of crane operator performance comparing PD-control and input shaping. In: *Proceedings of the 2011 American Control Conference*. San Francisco: IEEE, 2011, pp. 545–550. ISBN 978-1-4577-0081-1. DOI: 10.1109/ACC.2011.5991506.
- [10] DUCHON, F. and A. BABINEC. *Snimace v mobilnej robotike*. 1st ed. Bratislava: Slovenska technicka univerzita v Bratislave, 2012. ISBN 978-80-227-3801-9.
- [11] LEW, J. Y., MOON S. SIMONOVA and S. KASCAK. A Simple Active Damping Control for Compliant Base Manipulators. *IEEE/ASME Transactions on Mechatronics*. 2001, vol. 6, iss. 3, pp. 305–310. ISSN 1941-014X. DOI: 10.1109/3516.951368.

About Authors

Marek PASKALA was born in 1977 in Komarno. He received the M.Sc. Degree in Mechatronics at Slovak Technical University in Bratislava. After graduation, he was with Slovak Academy of Science as a research worker. From 2005 to now he is as a research worker at the Department of Mechatronics and Electronics, at the University of Zilina. He received the Ph.D. degree in Automation from the same university in 2014. His research interest includes mechatronic systems and control of PLC systems.

Jozef SEDO was born in 1985 in Zilina, Slovakia. He graduated at the Faculty of Electrical Engineering, University of Zilina in 2011. He received his Ph.D. degree in Power Electrical Engineering in 2016. He is currently working as an assistant professor in the Department of Mechatronics and Electronics at University of Zilina. His research interests include Power Electronics, Mechatronics and Control Systems.

Anna KONDELOVA was born in Trstena, Slovakia in 1959. She received his M.Sc. from Slovak Technical University in Bratislava in 1983. After graduation, she was with Research Institute of Computer Science in Zilina as a research worker. From 1995 to 2001, she worked as a teacher at the Faculty of Mechanical Engineering at the University of Zilina. From 2001 till now, she is a teacher at Faculty of Electrical Engineering. She received the Ph.D. degree in Automation from the same university in 2013. Her research interests include electronics, microcomputer technology and embedded systems.